Int J Clin Exp Med 2015;8(10):17406-17417
www.ijcem.com /ISSN:1940-5901/IJCEM0013919

*Original Article*

# Pharmacokinetics of silybin nanoparticles in mice bearing SKOV-3 human ovarian carcinoma xenocraft

Xin-Lei Guan, Shu-Zhen Zhao, Rui-Jie Hou, Sheng-Hua Yang, Quan-Le Zhang, Shan-Lan Yin, Shi-Jin Wang

*Department of Obstetrics and Gynecology, The First Affiliated Hospital of Xinxiang Medical University, Weihui 453100, Henan Province, China*

Received August 3, 2015; Accepted October 4, 2015; Epub October 15, 2015; Published October 30, 2015

**Abstract:** The particle fabrication technique was used to fabricate monodisperse size and shape specific poly (lactide-co-glycolide) particles loaded with the silybin. Response surface methodology (RSM) using the central composite rotatable design (CCRD) model was used to optimize formulations of silybin nanoparticles. Further the optimized nanoparticles are characterized for particle size, zeta potential, surface morphology, entrapment efficiency, *in-vitro* drug release, silybin availability for tumor, plasma, lung, spleen, liver were determined. The significant findings were the optimal formulation of PLGA concentration 10 mg, PVA concentration 2000 and PET width of 6 gave rise to the EE of 88%, mean diameter of 223 nm and zeta potential of 25-mV. Release studies were investigated at pH 1.2 and pH 6.8. It was studied that lower the pH, faster the release of sylibin. The nanoparticles had~15-fold higher plasma exposure as measured by AUC contrasted to pure silybin. The nanoparticles had a 60% increase altogether tumor silybin presentation contrasted with pure silybin. Nanoparticles had higher silybin presentation in the spleen and liver contrasted with pure silybin suspension as expected for a nanoparticle formulation. The lung silybin presentation for the nanoparticle was additionally 2-fold higher than that of the pure silybin suspension. The results of pharmacokinetic parameters and oral bioavailability data exhibited that drug-nanoparticle complex could enhance the oral absorption of silybin and as well as the use of particles with smaller feature size may be preferred to decrease clearance by organs of the mononuclear phagocyte system.

**Keywords:** Silybin, nanoparticle, ovarian cancer, pharmacokinetics, response surface methodology

## Introduction

For the enhanced delivery of therapeutic and diagnostic agents especially to cancer, nano drug delivery system has been utilized which explores macromolecular and nanoparticle carriers. The advantages of the nanodrug delivery system were enhanced drug solubility, extended drug half-life, and passive targeting to solid tumors by the enhanced permeability and retention (EPR) effect [1, 2] with an ultimate goal of improved efficacy and decreased toxicity. Inspite of the success of nanomedicine, the percentage of nanoparticle reaching the tumor is still less and hence investigations on various other criteria that has impact on nanoparticle accumulation on tumor are warranted [3].

Microemulsions [4] and micelles [5] liposomes [6] emulsion/solvent evaporation [7] and nanoprecipitation [8] based polymeric particles are considered to be various formulation techniques in the preparation of nanoparitcles. However the particle compositions and fabrication techniques differ, nanoparticles for small molecule chemotherapy delivery are supposed to be similar enough [9-11]. Nanoparticles are designed for more than 10 nm to avoid renal clearance and extravasation to normal tissues, and smaller than 200 nm to reduce clearance by the liver and spleen of the mononuclear phagocyte system (MPS) [12, 13]. General patterns being built up in desired particle size for tumor accumulation, a few many studies are there to explain the role of particle size and shape on cellular uptake of particles [14-16]. Couple of studies have investigated the impact of particle shape on in vivo tumor accumulation. Geng et al showed that adaptable filomicelles have longer plasma flow times and avoid the MPS [17]. Chauhan et al have exhibited that a rod shaped particle with a small width has preferred tumor infiltration over spherical particles of comparative measurement [18].

Nonetheless, to date, the related impact of size and shape on chemotherapeutic tumor delivery has not been investigated. In this study, we connected the fabrication technology, which will be a delicate lithography process, to manufacture monodisperse populations of PLGA particles with high loadings of silybin [19]. Fabrication procedure produces size and shape particular particles that give the capacity to comprehend the part of size and shape on particle distribution in vivo [20]. With the nanoparticle shapes, we exhibited enhanced plasma pharmacokinetics and tumor delivery contrasted with the immaculate silybin suspension. Furthermore, contrasts in clearance can be seen for the nanoparticles recommending that shape may play a role in reducing clearance by the MPS and enhancing tumor delivery.

Silybin is one of the most seasoned medications considered here for liver malignancy. Despite the fact that it will be considered to be perfect for the treatment of liver malignancy, delivery to the liver still needs change. The adequacy of oral silybin as a hepatoprotective agent has marked down by its poor dissolvability, low bioavailability and low half-life [21]. Silybin should be managed every day to accomplish its blongings. Nanosized carriers encapsulating silybin can be taken up inactively in to Kupffer cells in the liver and can bring about expanded medication fixation in the liver, in this manner expanding helpful adequacy. They can bring about maintained systemic arriaval of sylibin for over a week, contingent apart different vaiables, in the wake of framing a depot in the Kupffer cells. In this way, rehashed day by day administration for sylibin can be evaded. Further, oral bioavailability issues with sylibin can be dodged since bioavailability is altogether higher after the administration of nanoformulations.

Then again, oxidative stress in Kupffer cells will be isknown to start the formation of liver fibrosis in numerous illnesses and consequently sylibin levels in these cells, if improved, can enormously enhance treatment with silybin. In this way, with this type of formulation, maintained release, change in bioavailability and additionaly improvement of biochemical assurance can be accomplished. Together, these mechanisms lead to increment in viability of treatment. Consequently, the goal of this study was to get ready and improve the biodegradable nanoparticles of silybin, and to assess their attributes like particle size, surface morphology, zeta potential, entrapment efficiency and drug loading efficiency lastly liver targetability and against disease viability taking after oral administration of nanoformulation of silybin.

## Materials and methods

### *Materials*

Poly (D, L-lactide-co-glycolide) (lactide:glycolide 85:15, 0.65 dL/g Inherent Viscosity at 30°C) and silybin were acquired from Sigma-Aldrich. Chloroform, acetonitrile and double distilled water for high performance liquid chromatography were obtained from Fisher Scientific. Poly ethylene terephthalate sheets (6" width) were purchased from KRS plastics. Fluorocur®, d = 200 nm; h = 200 nm; and d = 80 nm; h = 320 nm; prefabricated molds and 2000 g/mol polyvinyl alcohol coated PET sheets were obtained by Liquidia Technologies.

### *Particle fabrication*

In a "6 × 12" sheet of PET, a thin film of PLGA and silybin was deposited by spreading 150 μL of a 10 mg/mL PLGA and 10 mg/mL Doc chloroform solution using a #5 Mayer Rod and letting the solvent to evaporate. The PET sheet with the film was then put in contact with the patterned side of a mold and passed through heated nips at 130°C and 80 psi. From the PET sheet, the mold was then splitted passing through the hot laminator. The PET sheet was then coated with 2000 g/mol PVA and the patterned side of the mold was placed in contact. Passing this through the hot laminator to transfer the particles from the mold to the PET sheet, the mold was peeled from the PET sheet. The particles were removed by passing the Passing the PVA coated PET sheet through motorized rollers, the particles were removed. Water was applied to dissolve PVA to release the particles. The particles were purified and then concentrated by tangential flow filtration in order to remove excess PVA if any.

### *Experimental design*

Central composite rotatable design-response surface methodology (CCRD-RSM) was used to systemically investigate the influence of three critical formulation variables PLGA concentration, PVA concentration and PET width on particle size (nm), zeta potential (-mV) and encapsulation efficiency (%, w/w) of the prepared nanoparticles. For every component, the test reach was chosen on the premise of the after

effects of preliminary experiments and the feasibility of preparing the nanoparticles at the extreme values. The worth scope of the variables was PLGA concentration (×1) of 5 to 15, PVA concentration (×2) of 1000 to 2000 and PET width (×3) of 3 to 9. An aggregate of 20 tests were directed.

*Particle characterization*

SEM was made used in making pictures by pipetting a 50 μL sample of particle on a glass slide allowing the sample to dry and coat with 3 nm gold palladium alloy utilising a Cressington 108 auto sputter coater. Pictures were taken at an accelerating voltage of 2 kV using scanning electron microscopy. For size and zeta potential estimation, dynamic light scattering was used.

*Determination of entrapment efficiency*

Drug encapsulation efficiency of the prepared silybin nanoparticles were controlled by the accompanying techniques. Firstly, a certain volume of nanoparticle suspension was precisely taken, dissolved and diluted with anhydrous methanol. At that point, drug content in the resultant solution was determined by HPLC method and the computed drug amount was assigned as $W_{total}$. To focus the unencapsulated drug, level with volume of nanoparticle suspension was precisely taken and ultra-filtered by a filter membrane with molecular weight cut-off of 12 kDa. The ultra-filtrate was diluted with anhydrous ethanol and drug content in the resultant solution was analyzed under the same HPLC condition. The measure of free drug was assigned as $W_{free}$. Therefore, the drug encapsulation efficiency (EE) could be ascertained by the comparison EE (%) = (W_total-W_free)/W_total × 100 [22] Where $W_{total}$ was the total amount of drug, $W_{free}$ was the measure of unencapsulated drug.

*HPLC assay*

The concentrations of silybin in the silybin nanoparticles, and in vitro release or rats' plasma were resolved utilising a validated HPLC method. The HPLC system comprised of an isocratic pump, with UV detector. The column utilised was a C18. The mobile phase comprised of acetonitrile: methanol: 0.03 M $KH_2PO_4$ (3:49:48, v/v/v), and pH was changed in accordance with 3.0 with phosphoric acid. The flow rate was 1.0 mL/min. Silybin was measured at 288 nm.

*Sample extraction*

For the pharmacokinetic study, 20 μL of internal standard solution (2-naphthol, 0.5 μg/mL), 50 μL of 10% acetic acid solution, 2 mL ether, and 0.3 mL acetic ether were added to 200 μL of plasma and vortexed for 1 minute. The blend was then centrifuged at 4000 rpm for 10 minute, and after that the supernatant was taken and evaporated to dryness at 40°C under a delicate stream of nitrogen. The residue was reconstituted with 100 μL of the mobile phase, and 60 μL of the final solution was injected in the HPLC system.

*In vitro release studies*

*In vitro* release of silybin from the nanoparticles was performed by dialysis method. Silybin nanoparticles were dissolved in deionized water at a concentration proportionate to 2 mg/mL silybin. Pure silybin was dissolved in little methanol, then diluted with more deionized water (2 mg/mL), and used as a control. Five millilitres of the samples was transferred immediately to the dialysis bags. The bags were promptly put in 500-mL glass beakers containing 400 mL of the disintegration medium maintained at 37°C. The outer phase was stirred continuously with a magnetic stirrer and samples (1 mL) were taken at specific time intervals followed by renewal with 1 mL of new disintegration medium. The measure of drug in the samples withdrawn from the outer phase over a 12-hour period was determined by HPLC to describe the release of silybin. The disintegration medium was recreated gastric fluid (pH 1.2) and mimicked intestinal fluid (pH 6.8).

*SKOV-3 human ovarian carcinoma tumor xenografts*

The animal experiments were conducted in full compliance with local, national, ethical, and regulatory principles for animal care. All animals utilised were treated humanely. SKOV-3 human ovarian carcinoma cells were obtained from ATCC. These cells were propagated in culture and harvested in log-phase growth. Rats of 220-250 g in body weight were acclimated for 1 week prior to tumor cell injection. Subcutaneous administration of cells ($5.0 \times 10^6$ cells in 200 μL 1 × PBS) into the right flank of each rat was made. Tumor volume was figured using the formula: tumor volume ($mm^3$) = ($w2 \times l$)/2, where w =width and l = length in mm of the tumor.

**Table 1.** Central composite design consisting of experiments for the study of three experimental factors in coded levels with experimental results

| Formulation | Coded Value Variables | | | Response Values | | |
|---|---|---|---|---|---|---|
| | $X_1$ | $X_2$ | $X_3$ | EE (%) | ZP (-mV) | PS (nm) |
| 1 | -1 | -1 | -1 | 80 | -31 | 250 |
| 2 | 1 | -1 | -1 | 81 | -28 | 270 |
| 3 | -1 | 1 | -1 | 90 | -36 | 290 |
| 4 | 1 | 1 | -1 | 85 | -31 | 320 |
| 5 | -1 | -1 | 1 | 87 | -28 | 252 |
| 6 | 1 | -1 | 1 | 83 | -30 | 280 |
| 7 | -1 | 1 | 1 | 93 | -26 | 282 |
| 8 | 1 | 1 | 1 | 89 | -29 | 312 |
| 9 | -1 | 0 | 0 | 94 | -07 | 307 |
| 10 | 1 | 0 | 0 | 91 | -12 | 302 |
| 11 | 0 | -1.682 | 0 | 89 | -24 | 360 |
| 12 | 0 | 1.682 | 0 | 90 | -13 | 348 |
| 13 | 0 | 0 | -1.682 | 89 | -31 | 342 |
| 14 | 0 | 0 | 1.682 | 87 | -30 | 248 |
| 15 | 0 | 0 | 0 | 85 | -30 | 280 |

*Pharmacokinetic study*

42 days after tumor cell implantation, the pharmacokinetics of the silybin nanoparticle was contrasted with suspension of silybin in rats in a randomized two-period crossover study after an oral dose comparable to 12 mg/kg silybin. The washout period between administrations was 1 week. Twelve male rats weighing 220-250 g housed on standard laboratory diet at an ambient temperature and humidity in air-conditioned chambers were used for this study. Prior the experiments the rats were fasted overnight. After administration, about 0.4 mL of blood was collected through the orbital sinus vein into heparinized tubes at the predefined times. The plasma obtained by centrifugation (10 minutes, 4000 rpm 1 788.8 g) was stored at -20°C until analysis. Cryopreservation vials was made used in preserving plasma and tissues. Preservation was made by snap freezing using liquid nitrogen. Tissues were stored at -80°C until analysis. Samples were processed for sum total (encapsulated + released) silybin using a protein precipitation method and analyzed by LC-MS/MS.

*Sample preparation and processing*

Total tissue and tumor weight was recorded at time of gathering. Entire tissue and tumors were snap frozen in liquid nitrogen and stored at -80°C until homogenized. To form homogenates, the intact tissues or tumors were thawed and sectioned. The sections were weighed and diluted in a 1:3 ratio with phosphate buffered saline (PBS) solution (assumes tumor and tissue has a density of 1 mg/mL). At long last, these blends were homogenized by placing zirconium oxide beads (15 small and 2 large) into 2 mL tubes at 3000 × g using a Precellys 24 homogenizer twice for 15 s each with a 5 s wait between each run. The resulting homogenates were snap frozen in liquid nitrogen and stored at -80°C until processed.

Calibration standards, quality control samples, and dilution control samples were prepared in identical framework that had exhibited no interfering components by the addition of 10 µL of a 10 × solution of analyte in acidified methanol (0.1% v/v acetic acid). Dilution controls and diluted unknown samples were diluted 1:10 (10 µL sample + 90 µL appropriate matrix) prior to any processing. All samples, standards, and controls were processed as follows: 100 µL of plasma or, tumor or tissue homogenate was pipetted into a 96-well silanized glass insert, protein-precipitated with the addition of 100 µL of a 50:50 mixture of methanol:acetonitrile containing the internal standard solution, vortexed for 1 min, and centrifuged for 15 min at 3000 × g at 4°C. The supernatants were analyzed by liquid chromatography with detection by tandem mass spectrometry with no further manipulation needed.

*Liquid chromatography tandem mass spectrometry (LC-MS/MS)*

LC-MS/MS analytical method was utilised for the quantification of analytes. Shimadzu solvent delivery system and an Applied Biosystems API 4000 triple quadruple mass spectrometer with an APCI ion source were used for these analytical studies. Separation was accomplished using a C18, 30 × 2.0 mm column, with a 5 µm particle size.

*Pharmacokinetic analysis*

Pharmacokinetic analysis was performed by the non-compartmental method, using the Kinetica 4.4. $C_{max}$ and $T_{max}$ were observed as raw data. Area under the curve to the last measurable concentration (AUC0-t) was calculated by the linear trapezoidal method. Area under the curve extrapolated to infinity

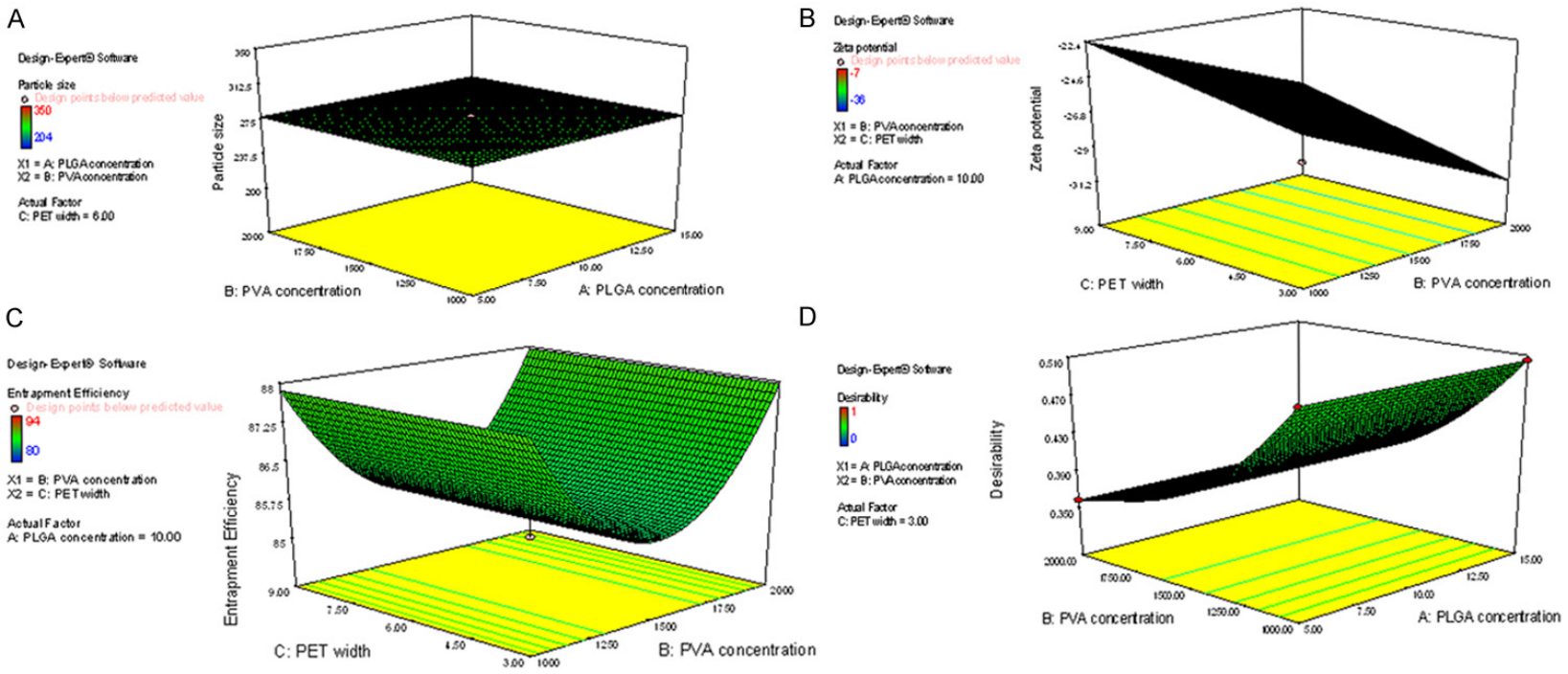


**Figure 1.** Three dimensional (3D) response surface plots showing the effect of the variable on the response. (A) The effect of PLGA and PVA concentration on the Particle size; (B) The effect of PVA concentration and PET width on the Zeta potential; (C) The effect of PET width and PVA concentration on Entrapment efficiency and (D) the overall desirability function.

**Table 2.** Comparison of experimental and predicted values under optimal conditions for final formulation

| PLGA concentration | PVA concentration | PET width | Particle size (nm) | Entrapment efficiency (%) | Zeta potential (-mV) |
|---|---|---|---|---|---|
| 10 | 2000 | 6 | | | |
| Predicted | | | 225 | 89 | 27 |
| Experimental | | | 223 | 88 | 25 |
| Bias (%) | | | 2% | 1% | 2% |
| Acceptance criteria = 2% | | | | | |
| Bias was calculated as (predicted value-experimental value)/predicted value × 100 | | | | | |

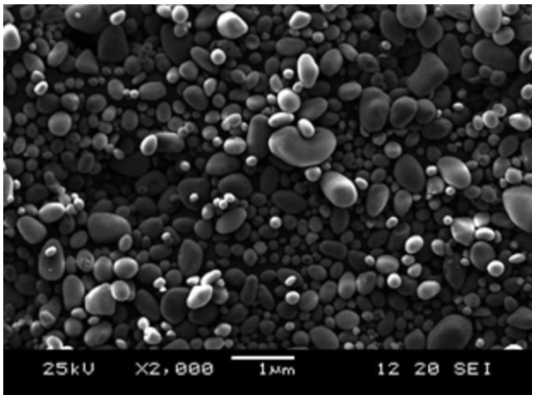


**Figure 2.** Scanning electron microscopy image of the silybin nanoparticle.

($AUC_{0-\infty}$) was calculated as AUC0-t + Ct/k, where Ct and k were the last measurable concentration and the elimination constant, respectively

*Statistics*

ANNOVA was used to analyse the data for statistical differences followed by Bonferroni's modified t test for multiple comparisons using GraphPad Prism. To determine the statistical significance, the confidence interval was set at 95%.

## Results

*Optimization of formula*

The central composite rotatable design-response surface methodology (CCRD-RSM) constitutes an alternative approach because it offers the possibility of investigating a high number of variables at different levels with only a limited number of experiments [23]. **Table 1** showed the experimental results concerning the tested variables on drug encapsulation efficiency, zeta potential, and mean diameter of particle size. A mathematical relationship between factors and parameters was generated by response surface regression analysis using Design-Expert® 7.0 software. The three-dimensional (3D) response surface graphs for the most statistical significant variables on the evaluated parameters are shown in **Figure 1**. The response surface diagrams showed that the higher the PLGA and PVA concentration larger is the particle size. Furthermore, the zeta potential increases significantly with the decreasing PVA concentration. The lack-of-fit was not significant at 95% confidence level. All the remaining parameters were significant at $P \leq 0.05$. The statistical analysis of the results generated the following polynomial equations:

$$EE=+88.44+2.52\times A+1.76xB-7.75\times AB-7.09\times B^2$$

$$ZP=+3.50-3.45\times A-0.12xC+2.75\times A^2+0.99\times C^2$$

$$PS=+151-58.38\times C+16.03\times C^2$$

where X1, X2 and X3 represent the coded values of the PLGA concentration, PVA concentration and PET width respectively. The fitting results indicated that the optimized nanoparticles with high EE, ZP and small mean diameter was obtained at the PLGA concentration of 10 mg/ml, PVA concentration of 2000 g/mol and PET width of 6, respectively. **Table 2** showed that the experimental values of the two batches prepared within the optimum range were very close to the predicted values, with low percentage bias, suggesting that the optimized formulation was reliable and reasonable. The overall desirability (D) 0.746 observed was represented graphically in **Figure 1**.

*Particle fabrication*

The nanoparticle preparation procedure makes exemptionally monodisperse particles as pictured by the SEM (**Figure 2**). The particles had

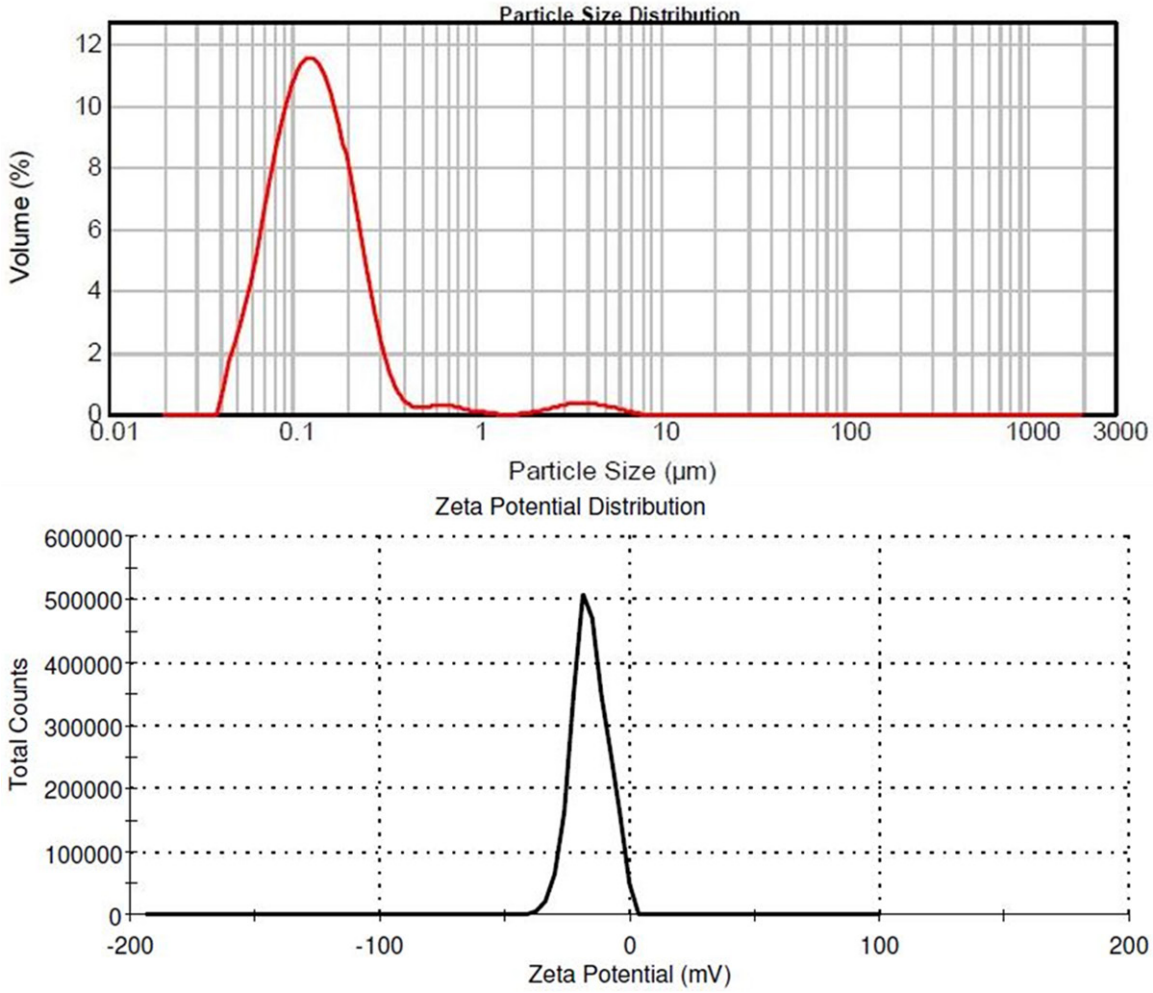


**Figure 3.** Particle size distribution and zeta potential of silybin nanoparticle.

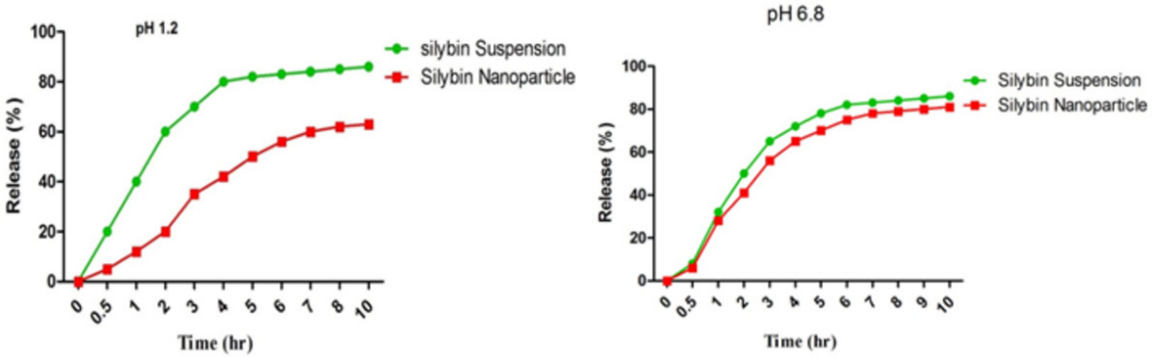


**Figure 4.** *In vitro* release of silybin from silybin nanoparticle compared with the diffusion of a silybin suspension in simulated gastric fluid, pH 1.2 and simulated intestinal fluid, pH 6.8.

somewhat negative zeta potential as a result of the PVA that remaining parts connected with the particle following harvesting and purification. Amid fabrication, the particles are transferred from the mold to PVA coated PET sheets. At the point, when the harvest sheet is dissolved with water during bead harvesting to release the particles from the sheet to solution,

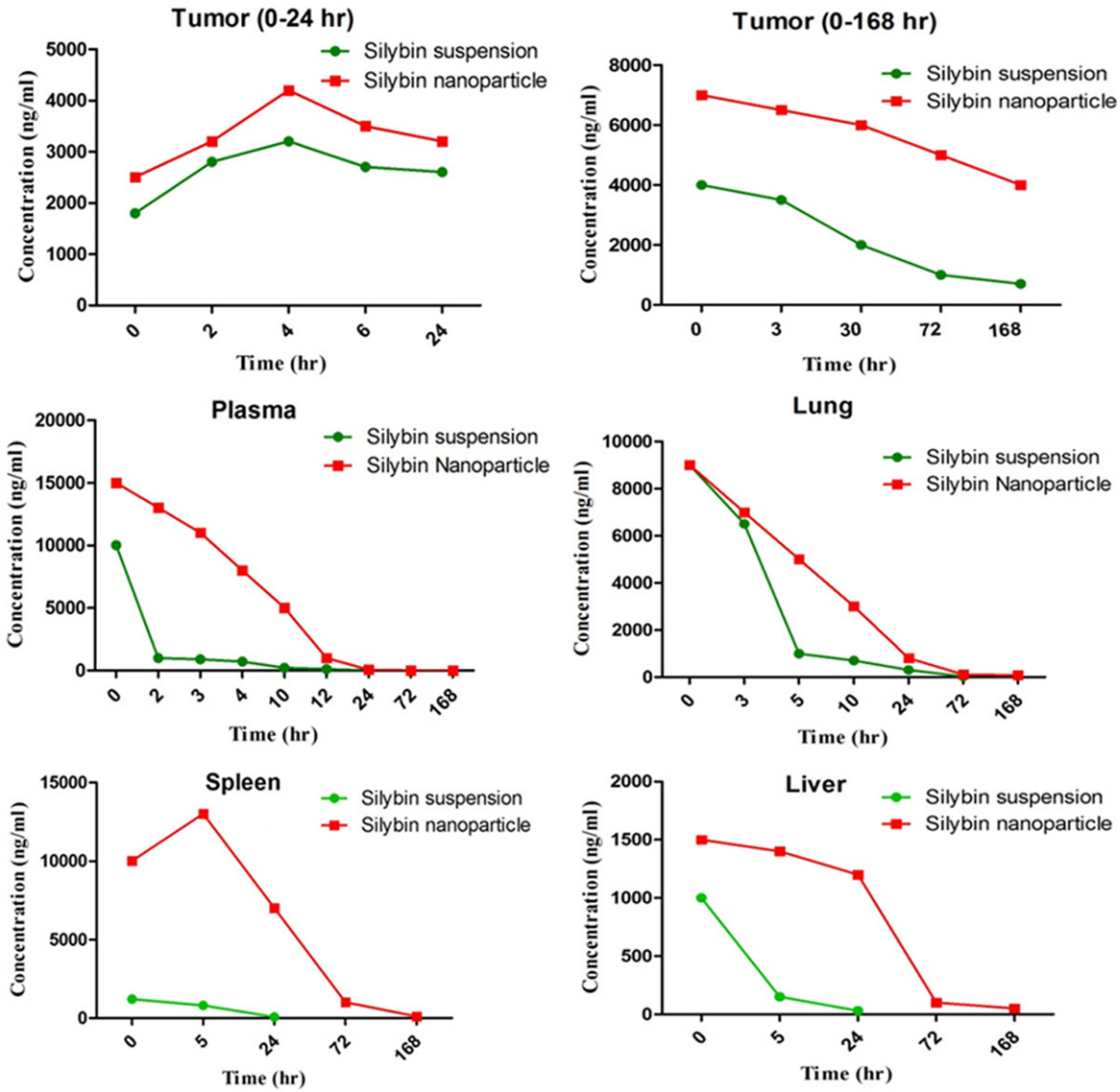


**Figure 5.** Silybin concentration versus time curve for Tumor (0-168 h), Tumor (0-24 h), Plasma, Lung, Spleen and Liver.

PVA is adsorbed onto the particle surface. This slight negative zeta potential may decrease nonspecific cellular uptake.

Particles were measured for size by DLS. Inspite of the non-spherical particle shapes are not perfect for DLS estimation, the recorded measurements for the nanoparticle were greater than 200 nm on an average. The mean particle size of silybin nanoparticles was 223 nm with a polydispersity index of 0.194 ± 0.016 (**Figure 3**). A narrow PI implies that the colloidal suspensions are homogenous in nature. The Zeta potential of the silybin nanoparticle was found to be -25 mV, and it is sufficiently high to form stable colloidal nanosuspension.

Additionally, the silybin w/w% loading is much higher in nanoparticle formulation. The silybin nanoparticles were loaded at a w/w% of 88%. Particles were washed with sterile water and concentrated by tangential flow filtration, which allowed some silybin to leach.

Additionally, the strength and stability of the drug-nanoparticle complex were investigated using *in vitro* release studies in simulated gastric fluid (pH 1.2) and simulated intestinal fluid (pH 6.8). Because the external electrostatic interaction was found to be the major mechanism for drug complexation by nanoparticles, we can expect that the strength of electrostatic interaction determines the drug release behav-

**Table 3.** Pharmacokinetic parameters of pure silybin suspension and silybin nanoparticle

| Specimen | Parameter | Unit | Formulation | |
|---|---|---|---|---|
| | | | Silybin suspension | Silybin nanoparticle |
| Plasma | $AUC_{0-t}$ | ng/ml.h | 5342 (0-24 h) | 132122 (0-24 h) |
| | $C_{max}$ | ng/ml | 10120 ± 523 | 52220 ± 526 |
| | CL | mg/ml | 1652 | 75 |
| | Vd | mg/ml | 8216 | 468 |
| Tumor | $AUC_{0-t}$ | ng/ml.h | 212612 (0-168 h) | 322848 (0-168 h) |
| | | | 58226 (0-24 h) | 86412 (0-24 h) |
| | $C_{max}$ | ng/ml | 3246 ± 496 | 4028 ± 38 |
| | $T_{max}$ | h | 1 | 1 |
| Liver | $AUC_{0-t}$ | ng/ml.h | 10228 (0-24 h) | 60224 (0-24 h) |
| | $C_{ma}x$ | ng/ml | 14268 ± 1024 | 10120 ± 1246 |
| Spleen | $AUC_{0-t}$ | ng/ml.h | 12196 (0-24 h) | 228178 (0-24 h) |
| | $C_{max}$ | ng/ml | 2942 ± 502 | 12012 ± 528 |
| Lung | $AUC_{0-t}$ | ng/ml.h | 12224 (0-72 h) | 38422(0-72 h) |
| | $C_{max}$ | ng/ml | 4120 ± 460 | 4928 ± 608 |

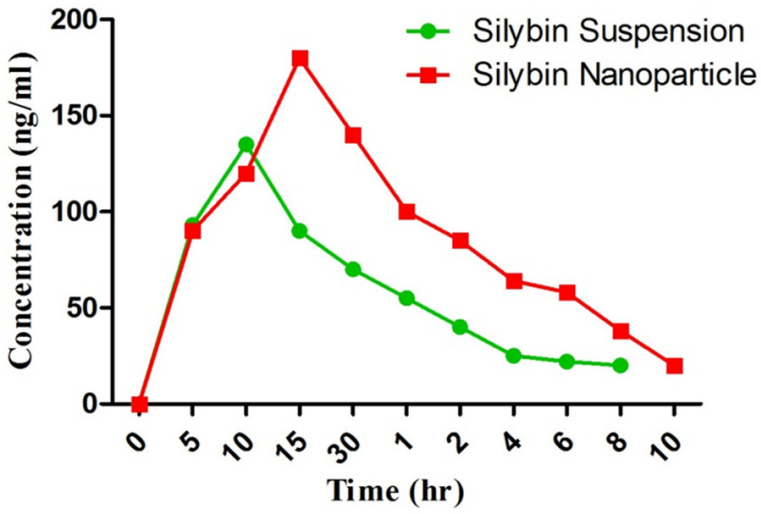


**Figure 6.** Silybin concentration versus time plot after a single oral dose of 12 mg/kg equivalent silybin nanoparticle and pure silybin suspension.

ior from nanoparticles. The release of silybin from nanoparticle matrixes should be faster in lower pH conditions. As it can be seen from **Figure 4**, the lower the pH values the faster the release rate of silybin. This is due to the availability of positively charged proton to interact with the phenolic hydroxyl group of silybin molecules, which reduces the electrostatic interactions between the nanoparticle matrix and the drug, thereby increasing the release rate of silybin from nanoparticles. Alternatively, the positive charge of nanoparticles, which increase the polarity of the interior cavities of nanoparticles, would contribute to the distinct release behavior of silybin in different pH conditions. The differences of drug release rate in different dissolution media can be correlated with a combination effect of the ionization state of the drug and the nanoparticles. These results strongly suggested that electrostatic interaction might play an important role in release of drugs from nanoparticle matrixes.

*Pharmacokinetics of silybin nanoparticles*

Sum total (encapsulated and released) of silybin was measured for each organ. The concentration versus time profiles of silybin nanoparticle and pure silybin solution in plasma, tumor, spleen, liver and lungs are displayed in **Figure 5**. The pharmacokinetic parameters of silybin nanoparticles and pure silybin solution in plasma, tumor, spleen, liver and lungs are introduced in **Table 3**.

The nanoparticles had~15-fold higher plasma exposure as measured by AUC contrasted to pure silybin. The nanoparticles had~7-fold higher maximal plasma silybin concentration than the pure silybin suspension. The difference in $C_{max}$ was significantly higher for nanoparticles contrasted with pure silybin suspension. Furthermore, the volume of distribution was much lower for the nanoparticles compared to pure silybin. The Vd was again ~20-fold less than that of pure silybin. Encapsulation of silybin into nanoparticles also decreased the clearance by ~25-fold contrasted with pure silybin.

The nanoparticles had a 60% increase altogether tumor silybin presentation contrasted with pure silybin from 0 to 168 h. Also, the sily-

bin concentration at 24 h was higher for the nanoparticles contrasted with pure silybin suspension. This demonstrates that the silybin nanoparticles may have steady accumulation at the site of the tumor. The plasma AUCs for 0-24 h and 0-168 h of the nanoparticles are found to be much higher than that of the silybin suspension. Hence, for the same plasma exposure from 0 to 24 h, it increases the impression that the nanoparticle is more proficient at delivering silybin to the tumor than the suspension.

Nanoparticles had higher silybin presentation in the spleen and liver contrasted with pure silybin suspension as expected for a nanoparticle formulation. However, the nanoparticles had~4 fold higher silybin presentation in the spleen contrasted with the pure silybin suspension. The maximal spleen concentration was additionally higher for the nanoparticles contrasted with the pure silybin suspension. The spleen silybin concentration for the nanoparticles was likewise higher than that of the pure silybin suspension.

The liver silybin presentation for the nanoparticle was 2-fold higher than that of the pure silybin suspension for $AUC_{0-24}$ h. In any case, the maximal concentrations were not altogether distinctive.

The lung silybin presentation for the nanoparticle was additionally 2-fold higher than that of the pure silybin suspension. The nanoparticles likewise gave a higher maximal silybin concentration in the lungs contrasted with the pure silybin suspension, which was measurably huge.

The oral bioavailability of silybin from silybin nanoparticles was evaluated in rats and contrasted with that of silybin suspension. **Figure 6** demonstrates the mean silybin plasma concentration versus time plots of the silybin formulation. The otcome showed that silybin suspension was quickly retained through the rat gastrointestinal tract with a $C_{max}$ of 134.2 ng/mL at a $T_{max}$ of 10 minutes. The administration of silybin nanoparticles accomplished a $C_{max}$ of 182.4 ng/mL at a $T_{max}$ of 15 minutes, and the entire blood concentration of silybin declined more gradually than that following suspension of silybin.

A non-compartmental model can be utilised to fit the experimental data of both silybin nanoparticle and suspension of silybin with regression coefficients of 0.9747 and 0.9901, respectively. Calculated on the basis of the $AUC_{0-\infty}$ of each formulation, the oral bioavailability of silybin nanoparticle was around 178% as contrasted at that of silybin suspension.

The results of pharmacokinetic parameters and oral bioavailability data exhibited that drug-nanoparticle complex could enhance the oral absorption of silybin. Past studies affirmed that nanoparticles at lower concentrations might be potential and safe absorption enhancers for improving absorption of poorly absorbable drugs from the small intestine [24]. It has been proposed that nanoparticles diminish the transepithelial electrical resistance value by extricating the tight intersection of $CaCO_2$ cells [25]. The opening of tight intersection in the epithelium may expand the transport of drugs through a paracellular route. Moreover, it has been accounted for that nanoparticles are transported through a mix of the paracellular pathway and adsorptive endocytosis [26]. It appears that various compoment as opposed to a single mechanism-including paracellular transportation of drug-nanoparticle complex across epithelium, enhanced contact with epithelium, and improved retention through the adsorptive endocytosis procedure may add to the upgraded oral bioavailability of silybin by nanoparticles.

## Discussion

PLGA nanoparticles with monodisperse size and specific shape were prepared. These particles had very high loadings of silybin. With the surfactants utilised (polyoxyethylated castor oil and tween 80), the formulations may bring about unfriendly responses in other words, adverse reactions identified [27, 28]. Thus, injecting less non dynamic excipient with respect to dynamic drug may expand tolerability of the formulation, particularly as identified with infusion related reactions [29].

The silybin nanoparticles brought about much higher plasma exposures of silybin contrasted with pure silybin suspension. Encapsulation of silybin into nanoparticles keeps the silybin more restricted to the plasma compartment to consider longer circulation and therefore expanded tumor aggregation. Also, decreased dispersion to typical tissues may improve the tolerability of the nano formulation contrasted with pure silybin suspension. Moreover, the

nanoparticles had higher tumor silybin presentation. Subsequently, however distinctive particles may have longer flow times and higher plasma drug presentation. Since insignificant measure of dose contrasted with aggregate dosage controlled achieves the tumor, incremental changes to enhance tumor delivery and transport may end up being advantageous.

Shape determination might likewise help in diminishing nanoparticle clearance from MPS related organs such as the spleen and liver. The smallest measurement of the particle may be the deciding component of particle clearance. Along these lines, future molecule outline may be directed by picking little particle measurements for better tumor delivery and MPS avoidance.

Nonetheless, however particles with smaller diameter may be favoured for enhanced passive targeting applications, smaller particles will ordinarily have expanded drug release rates because of expanded surface to volume proportion. This probable clarifies the higher silybin levels for nanoparticles in the tumor from 0 to 24 h, however not from 0 to 168 h. Diminishing release rate might likewise be liked to keep silybin within the particle while the majority of particles are still circulating within the first 24 h after administration. Studies are presently on going to determine the effect of drug release rate on pharmacokinetics and biodistribution in particles of the same size that have varied release rate.

Manufacture of nanoparticles produces monodisperse particles of particular size and shape that consider the investigation of the impacts of size and shape on drug distribution. In this study, the impact of size on silybin pharmacokinetics was studied. The silybin nanoparticles brought about much higher silybin plasma levels furthermore extraordinarily diminished appropriation volume and clearance. The increment in silybin plasma presentation because of silybin nanoparticle encapsulation prompted expanded tumor silybin exposure. Moreover, the silybin nanoparticle had significantly less silybin exposure in the spleen and also the liver and lungs. The silybin nanoparticle may be favored for long circulation because of its smaller diameter to penetrate pores, which brings about avoidance of the MPS and higher tumor accumulation.

## Conclusion

Taking everything in to account, the solubility of silybin was incredibly improved in the vicinity of PLGA nanoparticle. Complex of silybin with nanoparticle prompted sustained release of the drug in vitro and enhanced bioavailability in vivo. Nanoparticle drug delivery offers several attractive features, such as its effectively controllable size, shape, expanding length, and surface functionality that permit us to change the nanoparticle according to the prerequisites, and make this compound perfect carrier in a considerable lot of the applications.

## Acknowledgements

The authors are thankful to the department for conducting this research.

## Disclosure of conflict of interest

None.

**Address correspondence to:** Shi-Jin Wang, Department of Obstetrics and Gynecology, The First Affiliated Hospital of Xinxiang Medical University, No. 88 Jiankang Road, Weihui 27200, Henan, P. R. China. Tel: 0086-373-4402251; Fax: 0086-373-4402251; E-mail: wangshijin876@hotmail.com

## References

[1] Matsumura Y and Maeda H. A new concept for macromolecular therapeutics in cancer chemotherapy: mechanism of tumoritropic accumulation of proteins and the antitumor agent smancs. Cancer Res 1986; 46: 6387-92.

[2] Maeda H, Wu J, Sawa T, Matsumura Y and Hori K. Tumor vascular permeability and the EPR effect in macromolecular therapeutics: a review. J Control Release 2000; 65: 271-84.

[3] Chrastina A, Massey KA and Schnitzer JE. Overcoming in vivo barriers to targeted nanodelivery. Wiley Interdiscip Rev Nanomed Nanobiotechnol 2011; 3: 421-37.

[4] Dong X, Mattingly CA, Tseng MT, Cho MJ, Liu Y and Adams VR. Doxorubicin and paclitaxel-loaded lipid-based nanoparticles overcome multidrug resistance by inhibiting P-glycoprotein and depleting ATP. Cancer Res 2009; 69: 3918-26.

[5] Kim SC, Kim DW, Shim YH, Bang JS, Oh HS and Wan Kim S. In vivo evaluation of polymeric micellar paclitaxel formulation: toxicity and efficacy. J Control Release 2001; 72: 191-202

[6] Needham D, Anyarambhatla G, Kong G and Dewhirst MW. A new temperature-sensitive liposome for use with mild hyperthermia: char-

acterization and testing in a human tumor xenograft model. Cancer Res 2000; 60: 1197-201.
[7] Doiron AL, Chu K, Ali A and Brannon-Peppas L. Preparation and initial characterization of biodegradable particles containing gadolinium-DTPA contrast agent for enhanced MRI. Proc Natl Acad Sci U S A 2008; 105: 17232-17237.
[8] Gu F, Zhang L, Teply BA, Mann N, Wang A and Radovic-Moreno AF. Precise engineering of targeted nanoparticles by using self-assembled bio integrated block copolymers. Proc Natl Acad Sci U S A 2008; 105: 2586-2591.
[9] Farokhzad O and Langer RS. Nanoparticle delivery of cancer drugs. Annu Rev Med 2011; 63: 185-98.
[10] Petros RA and DeSimone JM. Strategies in the design of nanoparticles for therapeutic applications. Nat Rev Drug Discov 2010; 9: 615-27.
[11] Yoo JW, Chambers E, Mitragotri S. Factors that control the circulation time of nanoparticles in blood: challenges, solutions and future prospects. Curr Pharm Des 2010; 16: 2298-307.
[12] Choi HS, Liu W, Misra P, Tanaka E, Zimmer JP and Itty Ipe B. Renal clearance of quantum dots. Nat Biotechnol 2007; 25: 1165-1170.
[13] Chen LT and Weiss L. The role of the sinus wall in the passage of erythrocytes through the spleen. Blood 1973; 41: 529-37.
[14] Champion JA and Mitragotri S. Shape induced inhibition of phagocytosis of polymer particles. Pharm Res 2009; 26: 244-9.
[15] Gratton SE, Ropp PA, Pohlhaus PD, Luft JC, Madden VJ and Napier ME. The effect of particle design on cellular internalization pathways. Proc Natl Acad Sci 2008; 105: 11613-11618.
[16] Sharma G, Valenta DT, Altman Y, Harvey S, Xie H and Mitragotri S. Polymer particle shape independently influences binding and internalization by macrophages. J Control Release 2010; 147: 408-412.
[17] Geng Y, Dalhaimer P, Cai S, Tsai R, Tewari M and Minko T. Shape effects of filaments versus spherical particles in flow and drug delivery. Nat Nanotechnol 2007; 2: 249-255.
[18] Chauhan VP, Popović Z, Chen O, Cui J, Fukumura D and Bawendi MG. Fluorescent nanorods and nanospheres for real-time in vivo probing of nanoparticle shape-dependent tumor penetration. Angew Chem Int Ed Engl 2011; 50: 11417-11420.
[19] Rolland JP, Maynor BW, Euliss LE, Exner AE, Denison GM and DeSimone JM. Direct fabrication and harvesting of monodisperse, shape-specific nanobiomaterials. J Am Chem Soc 2005; 127: 10096-100100.
[20] Jeong W, Napier ME and DeSimone JM. Challenging nature's monopoly on the creation of well-defined nanoparticles. Nanomedicine 2010; 5: 633-639.
[21] Owens DE 3rd and Peppas NA. Opsonization, biodistribution, and pharmacokinetics of polymeric nanoparticles. Int J Pharm 2006; 307: 93-102.
[22] Liu H and Gao C. Preparation and properties of ionically cross-linked chitosan nanoparticles. Polym Adv Technol 2009; 20: 613-619.
[23] Ahn JH, Kim YP, Lee YM, Seo EM, Lee KW and Kim HS. Optimization of microencapsulation of seed oil by response surface methodology. Food Chemistry 2008; 107: 98-105.
[24] Yulian L, Takeo F, Naoko K, Yuiko T, Mariko N and Dong Z. Polyamidoamine dendrimers as novel potential absorption enhancers for improving the small intestinal absorption of poorly absorbable drugs in rats. J Control Release 2010; 149: 21-8.
[25] Kolhatkar RB, Kitchens KM, Swaan PW and Ghandehari H. Surface acetylation of polyamidoamine (PAMAM) dendrimers decreases cytotoxicity while maintaining membrane permeability. Bioconjug Chem 2007; 18: 2054-2060.
[26] Kitchens KM, Kolhatkar RB, Swaan PW, Eddington ND and Ghandehari H. Transport of poly (amidoamine) dendrimers across Caco-2 cell monolayers: Influence of size, charge and fluorescent labeling. Pharm Res 2006; 23: 2818-2826.
[27] Dye D and Watkins J. Suspected anaphylactic reaction to Cremophor EL. Br Med J 1980; 280: 1353.
[28] Kadoyama K, Kuwahara A, Yamamori M, Brown JB, Sakaeda T and Okuno Y. Hypersensitivity reactions to anticancer agents: data mining of the public version of the FDA adverse event reporting system AERS. J Exp Clin Cancer Res 2011; 30: 93.
[29] Tije AJ, Verweij J, Loss WJ and Sparreboom A. Pharmacological effects of formulation vehicles: implications for cancer therapy. Clin Pharmacokinet 2003; 42: 665-85.